Bone Formation in a Local Defect around Dental Implants Coated with Extracellular Matrix Components

Raquel R.M. de Barros, DMD;* Arthur B. Novaes Jr., DDS, DSc;* Paula Korn, DMD;†
Adriana Queiroz, DMD;* Adriana L.G. de Almeida, BS;* Vera Hintze, Dr.rer.nat.;‡
Dieter Scharnweber, Dr.habil.;‡ Susanne Bierbaum, Dr.rer.nat.;‡ Bernd Stadlinger, MD, DMD§

ABSTRACT

Purpose: The coating of implant surfaces with components of the extracellular matrix offers an approach to influence peri-implant bone healing. In this study, bone healing around coated implants is analyzed in a peri-implant defect model.

Materials and Methods: Eight months after extraction of the premolar teeth, six dogs received 48 implants (eight per animal) in the mandible. Implant surfaces were sandblasted and acid-etched, and some were additionally coated with collagen type II and chondroitin sulfate (collagen/CS). On each side of the mandible, implants either had no peri-implant defect (control side) or a vertical defect of 5 mm in depth and 0.5, 1.0, or 2.0 mm in width. Implants healed submerged for 8 weeks. Fluorochrome staining, histology, and histomorphometry were used to analyze implant osseointegration.

Results: Fluorochrome labels showed an increased mineralization around collagen/CS-coated surfaces at 4 weeks ($p = .031$). Histomorphometry generally showed lower vertical and horizontal bone apposition with increasing gap size for both surface types. In gapless sites and 0.5-mm gaps, collagen/CS coated implants showed increased bone volume in areas directly adjacent to the implant, in comparison with uncoated implants ($p < .05$).

Conclusion: The width of the peri-implant gap influences peri-implant bone formation. Complete filling of all gaps by newly formed bone could not be observed around either surface. In proximity to the surface, implant surface coating by collagen/CS positively influenced bone formation.

KEY WORDS: animal model, biocompatible, coated materials, dental implants, extracellular matrix, histology, osseointegration

INTRODUCTION

Implant osseointegration is a biological process that passes through different phases of wound healing until new bone formation occurs.[1] The interactions between proteins, cells, and the implant surface consecutively influence new bone formation.[2] The modification of implant surfaces aims to stimulate peri-implant bone formation, enabling earlier osseointegration and higher levels of bone-to-implant contact. Aside from the modification of implant surface topography or surface chemistry, one physiological approach is the coating of implants with components of the extracellular matrix (ECM).[3–6] The ECM represents the implant's natural surroundings in bone.[7] If major structural and functional matrix components are applied as implant coatings, their interaction with cells can potentially activate signaling pathways that positively influence bone healing.[8–11] Type II collagen is a fibril-forming collagen that is expressed in cartilage during bone formation and bone healing.[12,13] Various studies have shown a high affinity of type II collagen for glycosaminoglycans such as chondroitin sulfate (CS), and interactions between CS

*University of São Paulo, Ribeirão Preto, São Paulo, Brazil; †Clinic of Oral & Maxillofacial Surgery, Technische Universität Dresden, Dresden, Germany; ‡Max Bergmann Center of Biomaterials, Technische Universität Dresden, Dresden, Germany; §Clinic of Cranio-Maxillofacial and Oral Surgery, University of Zurich, Zurich, Switzerland

Reprint requests: Dr. Arthur B. Novaes Jr., DDS, DSc, Faculdade de Odontologia de Ribeirão Preto, Universidade de São Paulo, Av. do Café, S/N, 14040-904, Ribeirão Preto, SP, Brasil; e-mail: novaesjr@forp.usp.br

DOI 10.1111/cid.12179

and bone morphogenetic proteins have also been described.[14,15] The application of such ECM components to implant surfaces might thus influence the accumulation of growth factors and their presentation to bone-forming cells.[16] Previous animal studies have shown increased bone formation for collagen type I/CS coatings compared with uncoated surfaces and pure collagen type I coatings.[5,17,18] These histomorphometric studies were performed in uncompromised sites, suggesting that such ECM coatings can increase bone apposition. However, the question arises of whether such results translate to compromised sites.

A locally compromised site may arise during immediate implant placement due to the discrepancy between the implant diameter and the extraction socket anatomy. Immediate placement is defined as implant placement into a tooth extraction socket without prior hard or soft tissue healing.[19] Therefore, only the apical bone area can grant sufficient support for appropriate primary stability.[20] This results in a coronal peri-implant gap. Depending on the size of the gap, osseointegration can be achieved with or without the use of bone replacement substances or membranes.[21,22] The peri-implant bone defect is commonly widest in the marginal part and necessitates osseous healing from the walls of the defect to the implant surface.[23] For distances up to 1.25 mm, spontaneous bone fill has been shown to occur within 4 months.[21] In the case of wider peri-implant marginal defects, various bone-regenerative techniques have been used in humans to encourage bone growth within these defects, including barrier membranes, tissue grafts, and combinations of bone allografts and bioresorbable collagen membranes.[22,24,25] Accordingly, the purpose of this histomorphometric study is to investigate whether a collagen type II/CS-coated surface can improve peri-implant bone formation for implants placed after osteotomies that result in marginal defects.

MATERIALS AND METHODS

Coating of Test Implants

Collagen type II from chicken sternal cartilage (Sigma-Aldrich, Schnelldorf, Germany) was dissolved at 1 mg/mL in 10-mM acetic acid overnight at 4°C. CS from porcine trachea (a mixture of 70% chondroitin-4-sulfate and 30% chondroitin-6-sulfate) was purchased from Kraeber (Ellerbek, Germany) and solubilized to 0.1 mg/mL in 50-mM Na_2HPO_4 and 11-mM KH_2PO_4, pH 7.4. The prepared collagen solution was mixed on ice with an equal volume of buffer containing CS. Then, collagen fibrillogenesis was allowed to take place overnight at 37°C. The resulting fibrils were centrifuged at 5,000 g for 15 minutes, suspended in phosphate-buffered saline to 2 mg/mL collagen and homogenized by ultrasound. Implants were then dip-coated in 250 µL of this solution for 5 minutes with gentle shaking, using 96-well plates with the implants suspended in the coating solution by fixing them to the lid. After this, implants were air-dried. Dip-coating and drying was repeated one more time. Implants were washed twice for 10 seconds in deionized water, air-dried, and sterilized by gamma irradiation at ≥25 kGy.

This irradiation dose was used because it is the standard for medical products recommended by the European Pharmacopoeia. Gamma irradiation is reported to impair the mechanical properties of collagen/CS materials[26] and increases the degradation of collagen.[27] Despite its damaging effects, it seems to be the sterilization method of choice for retaining the bone-inductive properties of collagen-based biomaterials, as has been demonstrated for demineralized rat bone.[28]

Furthermore, we propose that the damage to dry collagen/glycosaminoglycan matrices by 25 kGy gamma irradiation is minimal, as the binding behavior of collagen/heparin matrices with vascular endothelial growth factor remains unaltered.[29] The coating was performed at the Max Bergmann Center, Technische Universität Dresden, Germany.

Operative Procedure

This study was performed as a preclinical large animal model on six adult male mongrel dogs with an average weight of 30 kg. Prior to surgery, the animals' health was checked by a veterinarian. The animals showed intact jaws and dentition and no signs of intraoral or systemic infection. The regional ethics committee for animal research approved the study (protocol number 018/2009).

For surgeries, animal sedation was performed with atropine (0.05 mg/kg subcutaneously) and thiopentone (2.5% solution, 20 mg/kg intravenously). Incubation was performed using an endotracheal tube, and a mixture of halothane (0.5–2.0%) and N_2O/O_2 (1:1) was administered.

The animals underwent two surgical interventions. The first intervention was the extraction of the mandibular premolars on both sides of the mandible

following bilateral full-thickness flap elevation. Prior to extraction, the second to fourth premolars were sectioned buccolingually at the bifurcation. This separation allowed the extraction of the root fragments, avoiding any damage to the neighboring bony walls. The soft tissues were repositioned and sutured using absorbable 4-0 sutures.

After 8 weeks of healing, implant placement was performed. Animals received 20,000 IU penicillin and streptomycin (0.1 g/kg) the night before implant placement and a second dose after 4 days. Implant placement started with a horizontal crestal incision on both sides of the jaw, ranging from the distal region of the canine to the first molar, followed by buccal and lingual full-thickness mucoperiosteal flap elevation, as also performed earlier.[30] The alveolar processes of both sides were slightly flattened in order to receive four 3.5 mm × 9.5 mm implants per side.

All 48 implants had a sandblasted and acid-etched surface (Plus surface, Xive, Dentsply-Friadent, Mannheim, Germany). Twenty-four implants were coated with collagen type II and CS (test surface); 24 uncoated implants served as controls.

All 48 implants (8 implants per animal, 4 implants per mandibular quadrant) were placed 1.5 mm subcrestally according to the manufacturer's instructions. In order to create peri-implant defects, three specially designed step drills were used to enlarge the peri-implant area. The gap defects had a width of 0.5, 1.0, or 2.0 mm and a depth of 5 mm below the bone crest. Each side of the mandible randomly received only one type of surface, either reference or test. In order to take the changing anatomy of the mandible into account, the implant positions were as follows: (1) anterior, no gap; (2) medioanterior, 0.5-mm gap; (3) mediodistal, 1.0-mm gap; (4) distal, 2.0-mm gap. Following flap reposition, suturing was performed with resorbable sutures and implants healed submerged. During implant healing, the animals received a soft diet for 14 days. Suture removal was performed by that time. The animals were monitored on a regular basis, and tooth cleaning was performed after 4 weeks using an ultrasonic device (Figure 1).

Histological Procedure

After 8 weeks of submerged healing, the animals were sedated and sacrificed with an overdose of thiopental. The mandibles were resected, separated, and dissected into block biopsies. Further processing has been described earlier.[30] During processing the biopsies were fixed in 4% phosphate-buffered formalin (pH 7) for 10 days, transferred to a solution of 70% ethanol, and dehydrated in increasing concentrations of alcohol up to 100%, followed by infiltration and embedding in LR White resin (London Resin Company, Berkshire, UK).[30] Next, the specimens were hard-sectioned according to Donath and Breuner's technique.[31] Sections of a thickness of 30 µm were prepared using an Exakt cutting and grinding system (Exakt, Norderstedt, Germany). Histomorphometry was performed at one central section of each implant. Following fluorescence analysis, the sections were stained with toluidine blue.

Fluorochrome Labeling

Fluorochrome labeling was applied for the analysis of the degree of new bone formation over time. For this purpose, four different fluorescent bone markers were administered as follows: at first week after implant placement, 20 mg calcein/kg body weight, i.v. (Sigma, St Louis, MO, USA); at 2 weeks, 20 mg alizarin/kg body weight, i.v. (Sigma); at 4 weeks, 20 mg tetracycline/kg body weight, i.v. (Sigma); at 8 weeks, 20 mg calcein blue/kg body weight i.v. (Sigma).

Analysis

The histological sections were photographed and analyzed. This was performed utilizing a Leica DM LB2 microscope (Leica Microsystems, Wetzlar, Germany) linked to a Leica DC 300F video camera system (Leica Microsystems); Leica QWin software (Leica Microsystems) was used for image analysis.

Fluorescence Analysis

The fluorescence-microscopic analysis served to visualize the influence of implant surfaces on the dynamics of bone formation and remodeling. Fluorescence images were obtained along the long axis of each implant using the appropriate barrier filters, and image analysis was performed at ×10 magnification by one blinded examiner as previously described.[30] The following wavelength filters were used: I_3 for calcein green (excitation level 450–490 nm), $N_{2\text{-}1}$ for alizarin red (excitation level 515–560 nm), D for tetracycline (excitation level 355–425 nm), and A for calcein blue (excitation level 340–380 nm).

Bone formation over time (BD, %) as an indicator of the mineralization rate was assessed by administering

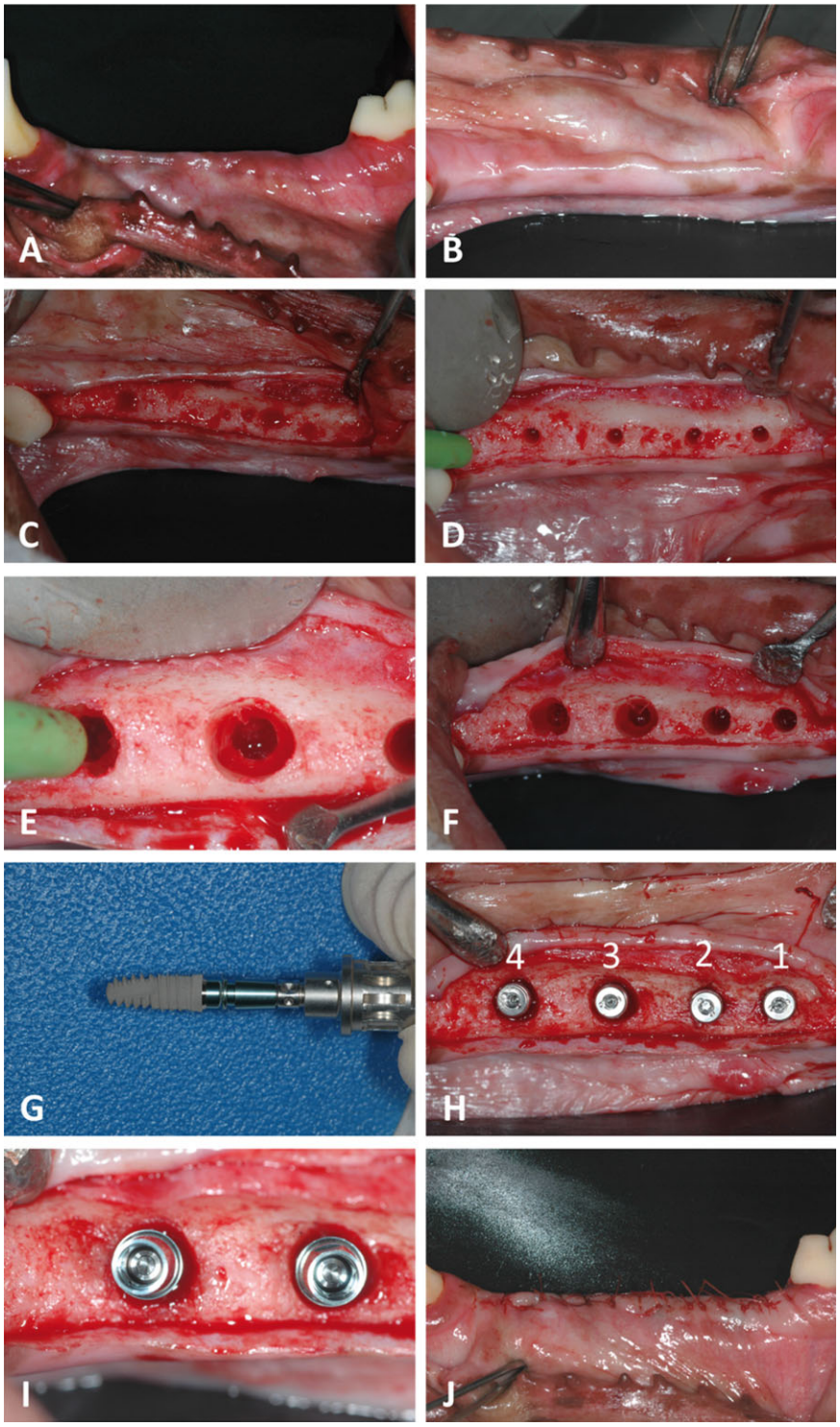

Figure 1 Clinical photographs. *A*, Implant site. *B*, Local anesthesia. *C*, Mucoperiosteal flap. *D*, Pilot drilling. *E*, Circumferential gap defects before implantation. *F*, From right to left, no gap defect (control) and gap defects of 0.5 mm, 1.0 mm, and 2.0 mm wide. *G*, Implant with reference surface. *H*, Four implants per mandibular side, with no gap (1, control) and gap defects of 0.5 mm (2), 1.0 mm (3), and 2.0 mm (4) wide. *I*, Implants in situ. *J*, Submerged healing.

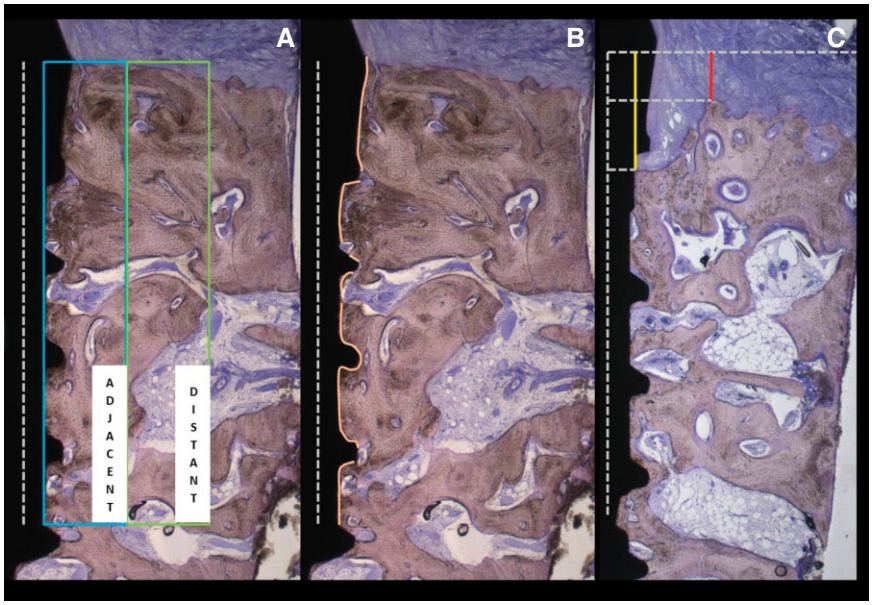

Figure 2 Histomorphometric parameters; toluidine blue staining, magnification ×2.5. *A*, Bone density in two rectangular regions of interest (adjacent and distant). White dotted line: original depth of the gap (5 mm). *B*, Bone-implant contact (both sides) over a length of 5 mm from the implant shoulder to the apical end of the gap. *C*, Linear vertical measurements of distance from implant shoulder to first bone-implant contact (yellow line) and distance from implant shoulder to level of crestal bone (red line); the latter indicates bone resorption or apposition.

fluorochromes at certain time points and calculating the percentage of fluorescence-stained bone area in relation to the total area formed within two regions of interest (ROIs) for each section on each implant side (left and right). Measurements were performed in the ROI directly adjacent to the implant (adjacent ROI) and in a ROI of identical shape neighboring the adjacent ROI at further distance from the implant (distant ROI). Each ROI had a rectangular shape (Figure 2), and adjacent ROIs included the various peri-implant defects (0.5, 1.0, or 2.0 mm in width and 5 mm in distance from the implant shoulder). The ROIs' length matched the apicocoronal depth of the gaps to be bridged. For gapless control sites, adjacent ROIs had a width of 0.5 mm and a length of 5 mm, analogous to the 0.5 mm–defect sites.

Histomorphometry

The histomorphometric analysis was performed at ×10 magnification by one blinded examiner. All parameters were measured on both sides of the implant (left and right) and are defined in the following as described in prior work.[30]

Histological bone density (BD, %) was evaluated within two ROIs (adjacent, distant) for every implant, as with the fluorescence measurement. The bone density was defined as being the percentage of mineralized bone in relation to the total ROI area. In adjacent ROIs, the implant groove area was subtracted. In the adjacent ROI, the percentage of newly formed bone was additionally measured.

Bone-to-implant contact (BIC, %) was determined for an area measuring 5 mm from the implant shoulder to the apical end of the gap, where the percentage of mineralized bone in direct contact with the implant surface was recorded.

Vertical bone resorption or IS-BIC (implant shoulder to first bone-to-implant contact, mm) in the peri-implant area was measured in a linear vertical plane as an assumed line from the implant shoulder to the most coronal bone-to-implant contact.

Another linear measurement was taken from the implant shoulder to bone crest level (IS-BC, mm) to evaluate bone resorption or apposition (see Figure 2).

The horizontal bone apposition (HBA, mm) within the three peri-implant defect types was determined by a linear horizontal measurement. Two parameters were assessed on both sides of every implant: complete resorption of the crestal bone (CR) and the full bone refill (BR) of the defect. This assessment was performed from the most cervical point of the defect to the bone

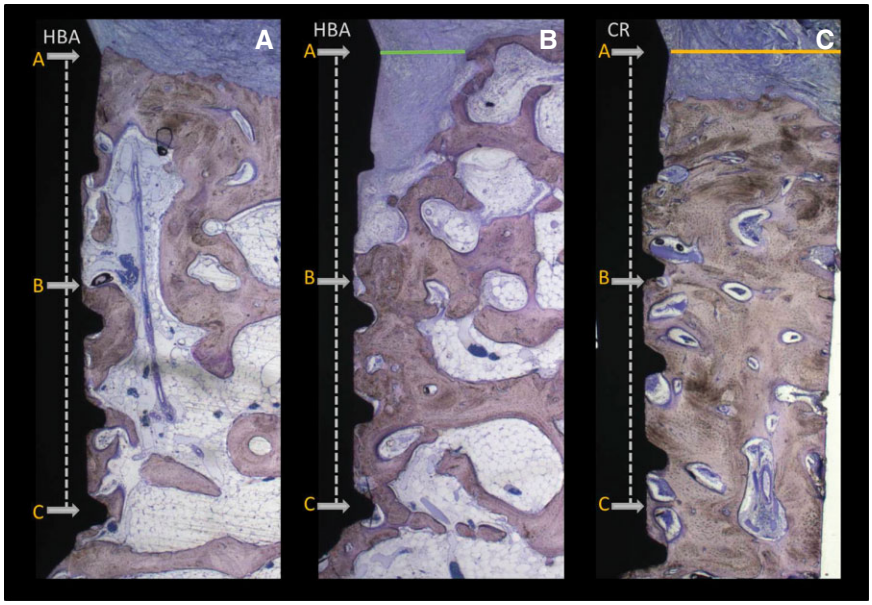

Figure 3 Linear horizontal measurements of the distance to bone at three points: "A," the most cervical point of the defect; "B," the midpoint of the defect; "C," the most apical point of the defect. Toluidine blue staining, magnification ×2.5. *A* and *B*, Horizontal bone apposition with total (*A*) and partial (*B*) filling of the gap. *C*, crestal bone resorption.

(A), the midpoint of the defect to the bone (B), and the most apical point of the defect to the bone (C). The horizontal bone apposition was further quantified in millimeters for points (B) and (C). These measurements serve to illustrate the potential for defect resolution around an implant surface (Figure 3).

Statistics

The study was designed as a two-factorial design (surface effect/gap zone effect). Two different implant surfaces were compared in a peri-implant gap model with four different gap zones. The study setup followed a parallel design. The statistical planning was performed by the Department of Medical Informatics and Biometry, Technische Universität Dresden, Germany. Statistical analysis was performed with SigmaStat for Windows, version 3.5 (Systat Software Inc., Chicago, IL, USA). Mean values and standard deviations were calculated. The level of significance was defined at 5%. Data were tested for normality (Kolmogorov-Smirnov test), and nonparametric paired tests were used. The Friedman test (two-way ANOVA for ranks) was applied for intragroup analysis, and if this test showed a high significance, the paired comparisons were made using the Tukey test. Intergroup comparison was accomplished using the Wilcoxon test.

RESULTS

Clinical Results

Postoperative healing after both surgical interventions, extraction and implant placement, was uncomplicated. There were no signs of impaired healing. All 48 implants were fully submerged and could be included in the analysis.

Fluorescence Microscopy

Fluorescent bone markers allow for the quantification of intravital bone mineralization. The intravenously applied dyes bind to newly formed bone areas that are mineralized at the time of application. Using different labels, the examination of bone formation dynamics is thus possible. Fluorescence microscopy was used to visualize dynamic bone remodeling for all cases. The host bone did not incorporate labels (Figure 4).

Histomorphometry served to assess new bone formation by fluorescent marker quantification. The amounts of fluorescence-marked bone formed after administration of fluorochromes after certain time periods (1, 2, 4, and 8 weeks) in adjacent and distant ROIs as percentages of that in the combined ROIs illustrates new bone formation and the pattern of peri-implant healing and is an indication of the mineralization rate (Table 1 and Figures 5 and 6).

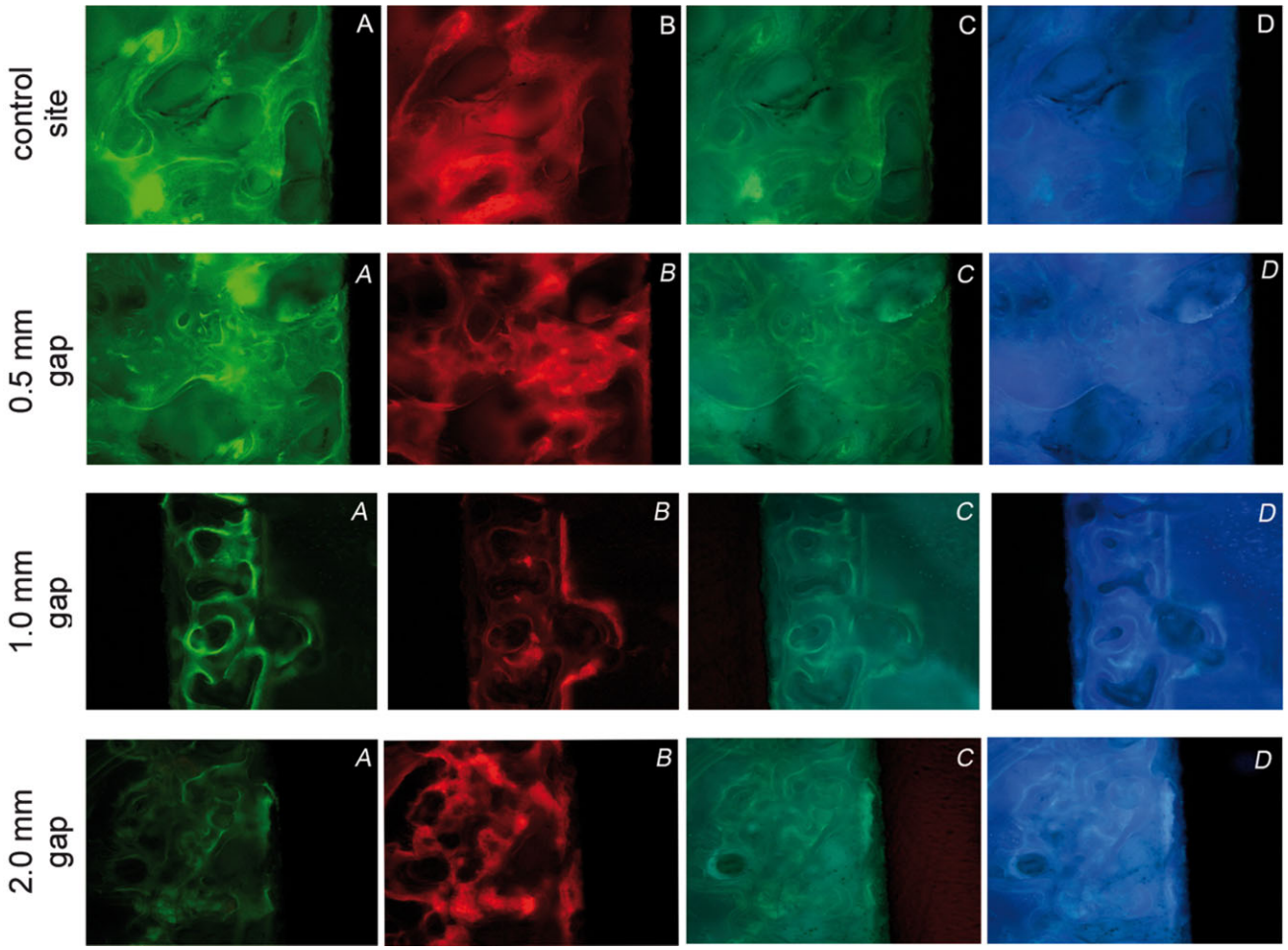

Figure 4 Fluorescence analysis. *A*, Calcein green showed well-defined green bands. *B*, Alizarin red appeared intense but smeared. *C*, Oxytetracycline showed delicate yellow-green lines. *D*, Calcein blue showed a dispersed pattern.

In the adjacent ROI, mineralization was between 3.87% (test surface, no gap) and 1.21% (control surface, 2.0-mm gap) at one week. Mineralization increased gradually in all groups by week 2 and week 4. The maximum values varied from 25.85% (test surface, no gap) to 13.50% (control surface, 2.0-mm gap) at 4 weeks. At 8 weeks, mineralization decreased in all groups to values between 9.31% (test surface, no gap) and 3.80% (control surface, 2.0-mm gap). Usually the test surface had slightly higher mineralization compared with the control surface, although significant differences between test (25.85%) and control surfaces (19.13%) with no gap could be detected only after 4 weeks ($p = .031$).

Distant ROIs showed generally lower mineralization, and the differences between the experimental groups were less pronounced. The dynamics over time were comparable with those in adjacent ROIs. At 4 weeks the maximum values were between 15.64% (control surface, no gap) and 5.57% (control surface, 2.0-mm gap).

In both adjacent and distant ROIs, mineralization, and thus bone formation, decreased with growing gap size. For collagen type II/CS coatings there was a slight positive effect on bone formation in adjacent ROIs, independent of the gap size detectable. There were no significant differences between the groups, except for the collagen type II/CS surface in gapless bone after 4 weeks, showing a significantly increased degree of mineralization compared with the uncoated control surface. The results for statistical intragroup comparisons based on the Tukey test are presented in Table 1.

Histology

Descriptive Histology. In general, all groups showed lamellar bone (old bone) as well as newly formed bone,

TABLE 1 Fluorescence Analysis Results

Area	Time	Surface	Newly Formed Bone (%) No Gap	0.5-mm Gap	1.0-mm Gap	2.0-mm Gap	$p^{\dagger}$
Adjacent	1 week	Test	3.87 ± 0.99[a]	2.97 ± 1.38[a,b]	1.97 ± 1.09[a,b]	1.37 ± 0.63[b]	.012*
		Control	3.57 ± 1.45	2.31 ± 1.62	2.21 ± 1.11	1.21 ± 0.70	.056
		$p^{\ddagger}$	1.000	.844	.438	1.000	
	2 weeks	Test	12.37 ± 3.68[a]	7.57 ± 3.36[a,b]	6.49 ± 2.67[a,b]	4.16 ± 1.96[b]	.014*
		Control	9.13 ± 4.30	6.70 ± 4.21	6.60 ± 3.71	3.54 ± 2.60	.050
		$p^{\ddagger}$	.219	.688	.438	1.000	
	4 weeks	Test	25.85 ± 5.13[a]	19.51 ± 5.64[a,b]	15.89 ± 2.57[a,b]	14.71 ± 3.48[b]	.012*
		Control	19.13 ± 5.75	16.66 ± 5.07	14.81 ± 6.49	13.50 ± 8.27	.060
		$p^{\ddagger}$	*.031*	.438	.563	.625	
	8 weeks	Test	9.31 ± 3.18	7.15 ± 2.76	6.22 ± 2.96	5.05 ± 3.97	.050
		Control	8.85 ± 2.98	5.90 ± 1.47	6.03 ± 3.09	3.80 ± 2.08	.125
		$p^{\ddagger}$	.844	.219	.844	1.000	
Distant	1 week	Test	1.24 ± 0.76	1.70 ± 1.78	1.16 ± 1.10	0.64 ± 0.34	.591
		Control	1.47 ± 0.54[a,b]	1.74 ± 0.79[a]	1.12 ± 0.68[a,b]	0.64 ± 0.42[b]	.026*
		$p^{\ddagger}$	.438	1.000	1.000	1.000	
	2 weeks	Test	5.07 ± 2.36	3.98 ± 3.12	3.34 ± 2.12	1.67 ± 0.87	.392
		Control	4.67 ± 2.60[a]	5.01 ± 1.76[a,d,e]	2.66 ± 1.51[b,d,f]	1.98 ± 0.83[c,e,f]	.017*
		p	.313	.438	.313	.448	
	4 weeks	Test	12.78 ± 5.33	10.34 ± 5.30	9.43 ± 4.09	8.14 ± 5.46	.896
		Control	15.64 ± 5.46[a]	12.59 ± 3.67[a]	8.98 ± 4.42[b]	5.57 ± 3.50[c]	.001*
		p	.094	.156	.844	.625	
	8 weeks	Test	6.00 ± 1.73	5.62 ± 1.80	4.98 ± 2.78	4.13 ± 1.85	.266
		Control	9.12 ± 5.36[a,b]	6.58 ± 2.69[a]	4.22 ± 2.25[a,b]	1.83 ± 1.02[b]	.010*
		p	.438	.523	.844	.125	

*$p < .05$.
†Friedman test (intragroup comparisons).
‡Wilcoxon signed-ranks test (between-group comparisons).
[a–f]Tukey test; different letters represent statistically significant differences.

which was observed mostly in the gap area. This new bone was characterized as fibrous tissue that sometimes appeared accompanied by a layer of osteoblasts (Figure 7). The surface between the new bone and the preexisting bone was evident in some specimens (Figures 8–11).

Bone Density. The BD for implants with the control surface in adjacent ROIs was between 49.67% (no gap) and 39.59% (2.0-mm gap). The percentage of newly formed bone in these adjacent ROIs was between 15.95% (no gap) and 12.22% (2.0-mm gap) without any significant differences within the groups. In distant ROIs the control surface showed a lower BD, between 45.68% (no gap) and 36.83% (2.0-mm gap) compared with the adjacent area. Around control surfaces, the size of the gap had no significant influence on BD in adjacent or distant ROIs.

Test surfaces showed an adjacent BD ranging from 65.47% (no gap) to 39.87% (2.0-mm gap). Adjacent BD was significantly higher around test surfaces with no or a 0.5-mm gap compared with test surfaces with a 2.0-mm circumferential gap ($p = .003$). The percentage of newly formed bone in adjacent areas was between 20.93% (no gap) and 12.23% (2.0-mm gap), without significant intra- or intergroup differences. For the distant BD, there were no significant intragroup differences for the test surface.

The intergroup comparison of BD between test and control surfaces showed a significantly higher BD in adjacent areas for test surfaces in gapless bone and 0.5-mm gaps ($p = .031$) and in distant areas for test surfaces in gapless bone ($p = .030$) (Table 2).

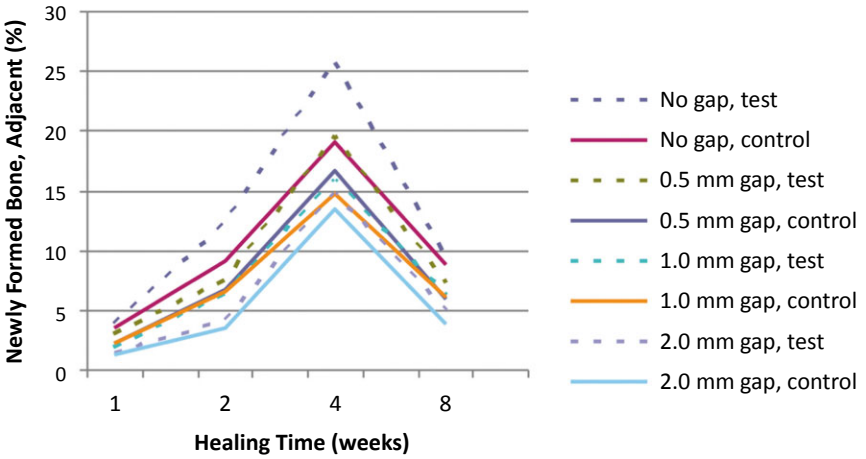

Figure 5 Percentages of newly formed bone in the adjacent regions of interest for control and test surfaces and the different peri-implant defects.

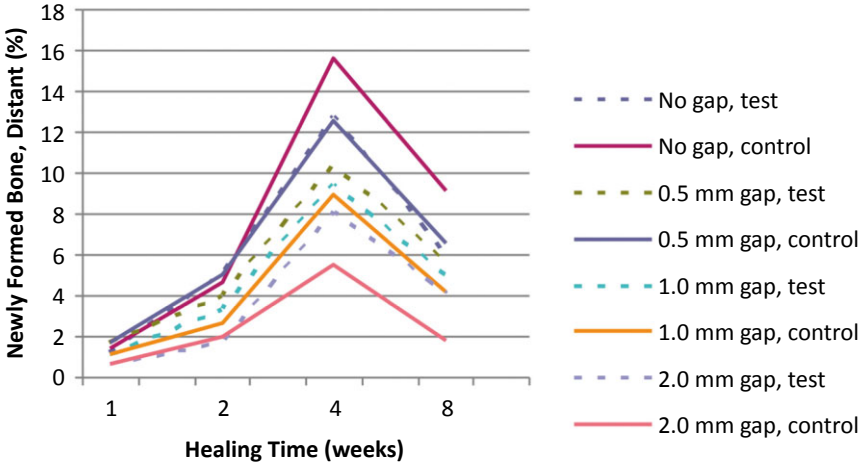

Figure 6 Percentages of newly formed bone in distant regions of interest for control and test surfaces and the different peri-implant defects. The size of the defect had an inversely proportional influence on the rate of bone formation.

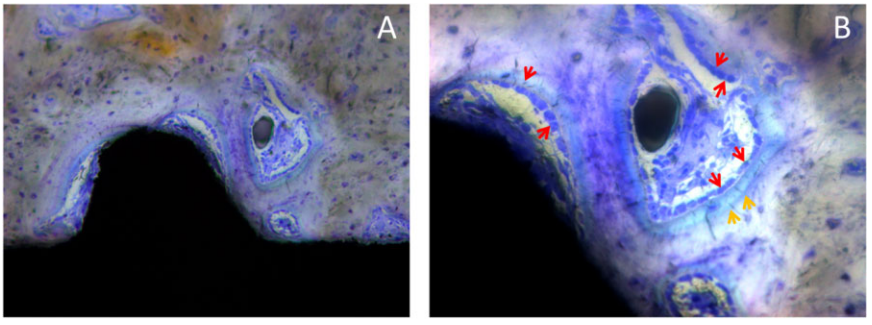

Figure 7 Histology. Bone formation on the implant surface. Toluidine blue staining. *A*, New bone in direct contact with the implant surface (implant spire), magnification ×20. *B*, Layer of osteoblasts (*red arrows*) and new bone deposition (*yellow arrows*), magnification ×40.

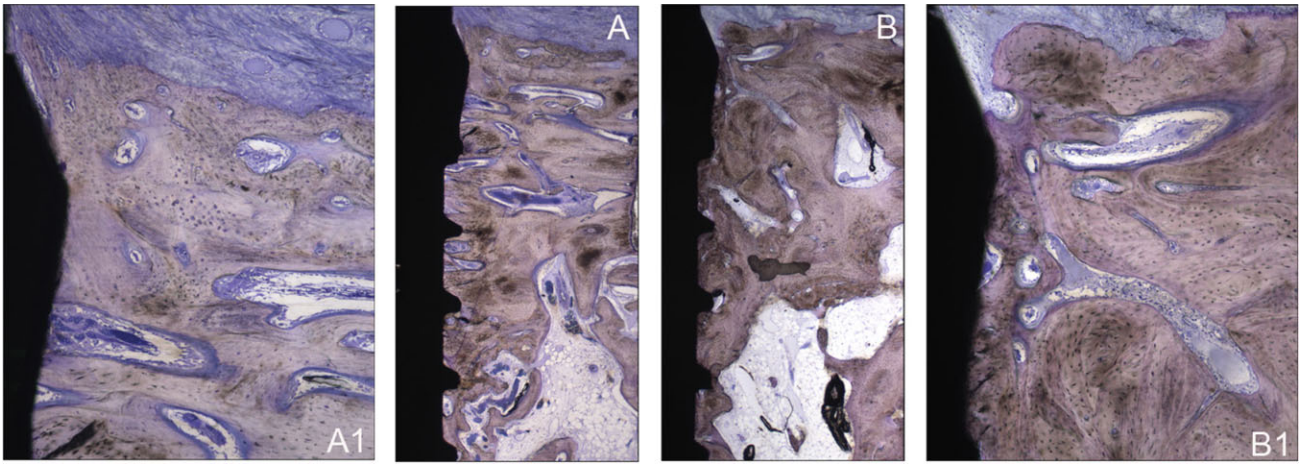

Figure 8 Histology: control sites (without defect). Both surfaces exhibited high levels of bone-implant contact and bone density. Bone formation above the implant shoulder was observed in both specimens. Toluidine blue staining. *A*, Control surface, magnification ×2.5. *A1*, Higher magnification (×10) of the area (square) outlined in *A*. *B*, Test surface, magnification ×2.5. *B1*, Higher magnification (×10) of the area (square) outlined in *B*.

Bone-Implant Contact. The BIC for control and test surfaces was inversely proportional to gap size. The values for control surfaces varied from 54.90% (no gap) to 30.77% (2.0-mm gap) with no significant differences. Test surfaces showed a slightly higher BIC, from 65.54% (no gap) to 34.77% (2.0-mm gap), compared with control surfaces. The combination of test surfaces and a 2.0-mm gap had a significantly lower BIC compared with the same surface without a circumferential gap ($p = .046$). The intergroup comparison between test and control surfaces did not show significant BIC differences in gapless or gap sites (see Table 2).

Implant Shoulder to Bone-Implant Contact. The distance from implant shoulder to the first bone-implant-contact for control surfaces was at least 1.08 mm (no gap) and at most 2.98 mm (2.0-mm gap). Implants with no gaps and those with 0.5-mm gaps displayed similar distances (1.25 and 1.24 mm). The difference in IS-BIC within the control surface group between 1.0-mm and 2.0-mm gaps was statistically significant ($p = .029$).

Test surfaces generally showed a lower IS-BIC distance compared with control implants. IS-BIC ranged from 0.72 mm (no gap) to 2.76 mm (2.0-mm gap).

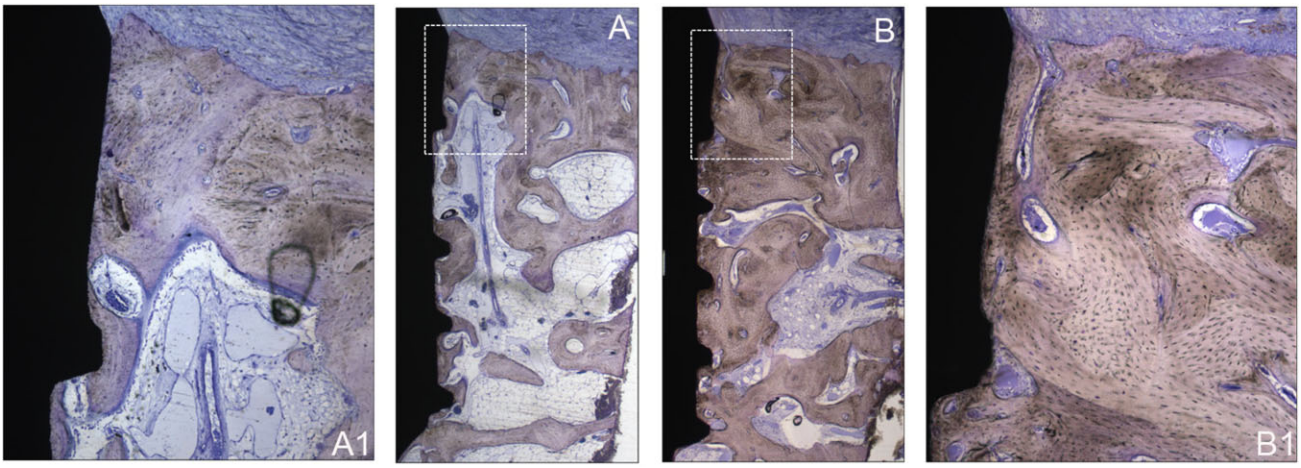

Figure 9 Histology: 0.5-mm gap sites. High levels of bone-implant contact for both specimens; complete defect fill, without vertical bone loss of the proximal bone crests. Toluidine blue staining. *A*, Control surface, magnification ×2.5. *A1*, Higher magnification (×10) of the area (square) outlined in *A*. *B*, Test surface, magnification ×2.5. *B1*, Higher magnification (×10) of the area (square) outlined in *B*. Note better bone density on the test surface compared with the control surface (observe the number of marrow spaces).

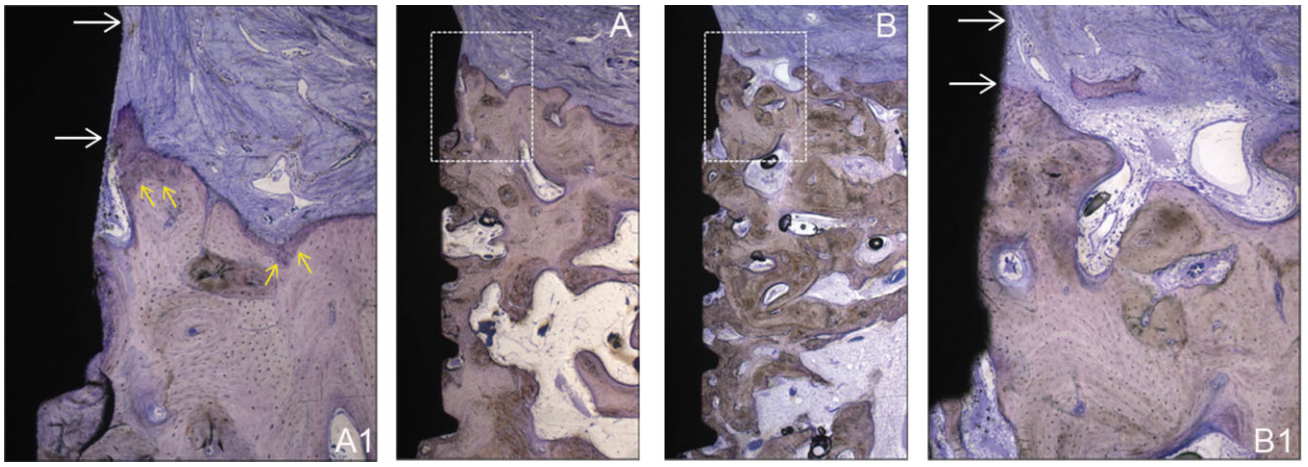

Figure 10 Histology: 1.0-mm gap sites. Vertical bone loss was observed in both specimens, being more pronounced on the control surface, as evidenced by the distance between the *white arrows*. The *yellow arrows* indicate the difference between the preexisting bone and the newly formed bone (strong color). Toluidine blue staining. *A*, Control surface, magnification ×2.5. *A1*, Higher magnification (×10) of the area (square) outlined in *A*. *B*, Test surface, magnification ×2.5. *B1*, Higher magnification (×10) of the area (square) outlined in *B*.

For test surfaces, a gap size of 2.0 mm led to significantly higher IS-BIC values compared with no gap or a 0.5-mm gap ($p = .007$). The intergroup comparison between test and control surfaces did not show significant IS-BIC differences for gapless or gap sites (see Table 2).

Implant Shoulder to Crestal Bone. For all control surfaces, vertical bone loss was detectable. This means the crestal bone level was lower than the implant shoulder. Larger gap sizes showed a lower level of crestal bone. The group without a gap showed a mean IS-BC value of –0.06 mm, while for the group with 2.0 mm gaps the value was –0.72 mm.

Test surfaces with circumferential gaps also had vertical bone loss, but to a lower degree, from –0.25 mm (0.5-mm gap) to –0.56 mm (2.0-mm gap), compared with control surfaces. For test surfaces the absence of a gap defect led to a vertical bone gain of 0.20 mm.

For IS-BC, intra- (gap size) and intergroup (test/control surface) comparisons showed no statistically significant differences (see Table 2).

TABLE 2 Intragroup Analysis of Bone Density, Bone-Implant Contact, and Vertical Bone Apposition

		Bone Density (%)				Vertical Bone Apposition	
Surface	Gap (mm)	Adjacent (Total)	Adjacent (New Bone)	Distant (Total)	Bone-Implant Contact (%)	IS-BIC (mm)	IS-BC (mm)
Test	None	65.47 ± 12.92*	20.93 ± 13.30	57.43 ± 12.03	65.54 ± 16.95‡	0.72 ± 0.67§	0.20 ± 0.88
	0.5	60.73 ± 14.59†	18,00 ± 8.34	48,05 ± 12.66	60.10 ± 16.80	0.83 ± 0.96¶	–0.25 ± 0.90
	1.0	49.42 ± 8.77	13.84 ± 3.71	44.74 ± 12.23	44.64 ± 13.65	1.69 ± 1.09	–0.43 ± 1.00
	2.0	39.88 ± 8.98*†	12.23 ± 2.89	37.48 ± 16.04	34.78 ± 16.30‡	2.76 ± 1.18§¶	–0.56 ± 0.55
Control	None	49.67 ± 15.53	15.95 ± 7.55	45.69 ± 8.42	54.90 ± 13.32	1.24 ± 0.68	–0.06 ± 0.82
	0.5	49.17 ± 13.85	14.09 ± 4.45	45.44 ± 6.63	52.41 ± 15.78	1.25 ± 1.06	–0.46 ± 0.61
	1.0	48.73 ± 4.17	13.39 ± 2.55	44.42 ± 7.32	40.72 ± 10.81	1.08 ± 0.86**	–0.47 ± 0.91
	2.0	39.59 ± 13.79	12.22 ± 3.83	36.83 ± 9.83	30.77 ± 26.34	2.98 ± 1.07**	–0.72 ± 0.96

Values are given as means ± SD.
Values with the same superscript are significantly different ($p < .05$).
*$p = .003$; †$p = .003$; ‡$p = .046$; §$p = .007$; ¶$p = .007$; **$p = .029$.
IS-BIC, distance between implant shoulder and bone-implant contact; IS-BC, distance between implant shoulder and crestal bone.

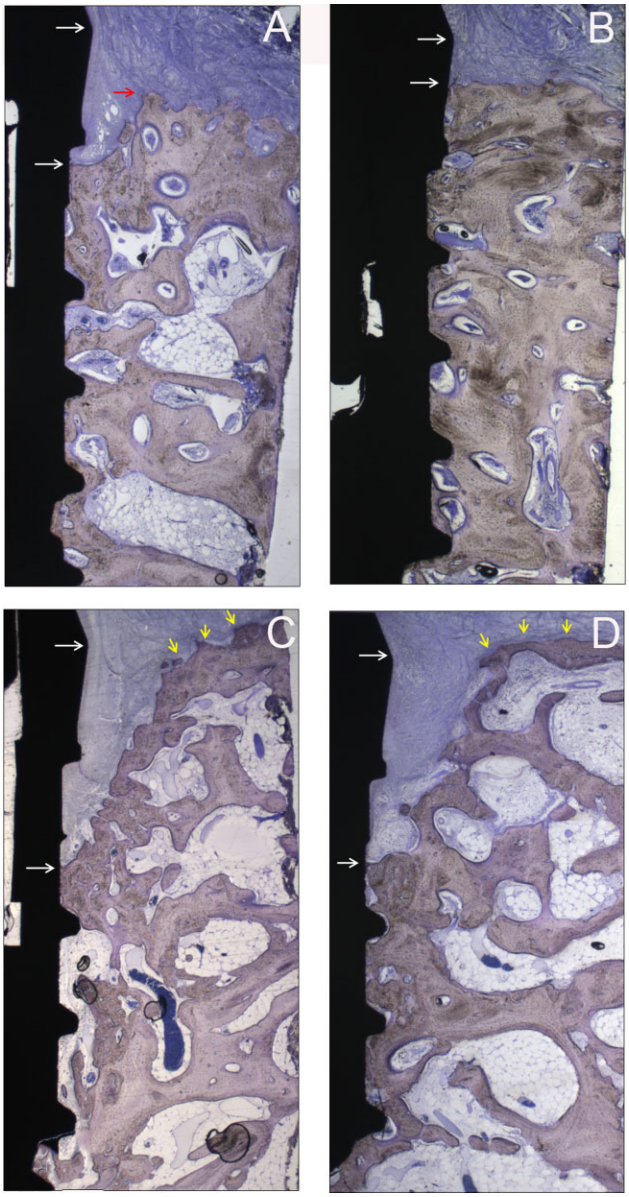

Figure 11 Histology: 2.0-mm gap sites. *A* and *C*, Control surface images, magnification ×2.5. *B* and *D*, Test surface images, magnification ×2.5. Toluidine blue staining. Bone healing in these gap defects resulted in two different situations. *A* and *B*, Vertical bone loss of the proximal bone crests, showing a lower crestal bone level but partial (A) or complete (B) bone fill of the 2.0-mm gap defect. *White arrows*: implant shoulder and first bone-implant contact BIC; *red arrow*: bone crest level, evidencing a residual defect. *C* and *D*, Residual defects, but with the bone crest levels (*yellow arrows*) appearing at the same level as the implant shoulders (*first white arrow*).

Horizontal Bone Apposition. The horizontal bone apposition was measured at three different levels of the defect by determining the distance between implant surface and adjacent bone. Additionally, two opposing phenomena were observed and measured: the complete resorption of the crestal bone (CR) in the vertical plane, or the full bone refill (BR) of the defect. The full refill implies that there is no more gap between the newly formed bone and the implant.

At the most cervical point (point A), test surfaces showed a higher amount of BR, up to a gap size of 1.0 mm, as well as a lower degree of CR compared with control surfaces.

In the middle of the defect (point B), the values for the distance between implant surface and bone ranged from 0.04 µm (test surfaces, no gap; control surfaces, 0.5-mm gap) to 0.33 µm (control surfaces, 2.0-mm gap). At the apical point of the defect (point C), a reduced distance between implant and bone was measured in almost all groups compared with point B. The values were between 0.01 µm (test surface, no gap) and 0.19 µm (test surface, 2.0-mm gap).

The horizontal bone apposition and the number of full BRs decreased with increasing defect size at point B and C. There was no CR at point B or C for any defect size. The influence of the implant coating was heterogeneous within the groups (Table 3).

Intergroup Analysis. The collagen type II/CS implant coating led to significantly ($p = .031$) higher values for BD in adjacent ROIs if there was no gap or a 0.5-mm gap compared with uncoated control surfaces under the same conditions.

BD in distant ROIs with no gap was also significantly higher ($p = .030$) for test surfaces compared with control surfaces. For the other parameters, BIC, IS-BIC, and IS-BC, no significant differences between the two implant surfaces were measurable (Table 4).

DISCUSSION

The osseointegration of microrough dental implants is the result of an osseous wound healing process that results in high implant success rates.[32] The development of new implant surfaces aims at further stimulating peri-implant bone formation, especially in the early healing phase. A critical point, especially in implant placement, can be the existence of a peri-implant gap as encountered during immediate placement, and influencing early healing may contribute to reducing this problem.

It is known from preclinical[33,34] and clinical studies[22,35] that a peri-implant gap can be bridged without the use of bone fillers or membranes, but peri-implant bone formation depends on the gap size.[36] Physiologically, the distance to be covered by primary

TABLE 3 Horizontal Bone Apposition inside Peri-Implant Defects

Gap Width (mm)	Implant Surface	Point A*		Point B†			Point C‡		
		CR (*n*)	BR (*n*)	Distance to Bone (μm)	CR (*n*)	BR (*n*)	Distance to Bone (μm)	CR (*n*)	BR (*n*)
No gap	Test	2	2	0.04	0	9	0.01	0	10
	Control	3	1	0.07	0	7	0.05	0	10
0.5	Test	4	2	0.05	0	9	0.03	0	9
	Control	5	1	0.04	0	11	0.04	0	8
1.0	Test	6	2	0.06	0	9	0.09	0	6
	Control	7	2	0.06	0	6	0.07	0	8
2.0	Test	10	0	0.23	0	3	0.19	0	4
	Control	10	1	0.33	0	6	0.18	0	6

Measurements were made for a total of 12 specimens (left and right sides of six implants).
*Most cervical point of the defect.
†Midpoint of the defect.
‡Most apical point of the defect.
CR, full crestal bone resorption; BR, full bone refill.

bone formation is limited,[37,38] which is due to the capacity of angiogenic sprouting to allow neovascularization and consecutive new bone formation.[39] In this study we investigated whether microrough implant surfaces coated with ECM components prevalent in growing bone (collagen type II, the collagen in osteochondral bone development, and chondroitin sulfate, the glycosaminoglycan component of ECM proteins associated with bone)[40] have the ability to positively influence bone formation in a peri-implant defect model with gaps of different dimensions (0.5, 1.0, 2.0 mm). We analyzed the implant surface influence on bone formation and gap bridging by analyzing new bone formation, bone density, bone implant contact, and the crestal bone level.

Dynamics of bone formation were visualized using sequentially administered fluorescent dyes, and this was not influenced by either coating or gap size. In all cases, the mineralization rate peaked at week 4 and decreased thereafter. This is in agreement with studies by Berglundh and colleagues,[1] who histologically analyzed the dynamics of bone formation around sandblasted and acid-etched surfaces and found newly formed mineralized tissue after 4 weeks, possibly indicating strong mineralization during that period. An earlier study by de

TABLE 4 Intergroup Analysis of Bone Density, Bone-Implant Contact, and Vertical Bone Apposition

Surface	Gap (mm)	Bone Density (%)			Bone-Implant Contact (%)	Vertical Bone Apposition	
		Adjacent (Total)	Adjacent (New Bone)	Distant (Total)		IS-BIC (mm)	IS-BC (mm)
Test	None	65.47 ± 12.92*	20.93 ± 13.30	57.43 ± 12.03‡	65.54 ± 16.95	0.73 ± 0.67	0.20 ± 0.88
	0.5	60.73 ± 14.59†	18.00 ± 8.34	48.05 ± 12.66	60.10 ± 16.80	0.83 ± 0.96	−0.25 ± 0.90
	1.0	49.42 ± 8.77	13.84 ± 3.71	44.74 ± 12.23	44.64 ± 13.65	1.69 ± 1.09	−0.43 ± 1.00
	2.0	39.88 ± 8.98	12.23 ± 2.89	37.48 ± 16.04	34.78 ± 16.30	2.76 ± 1.18	−0.56 ± 0.55
Control	None	49.67 ± 15.53*	15.95 ± 7.55	45.69 ± 8.42‡	54.90 ± 13.32	1.24 ± 0.68	−0.06 ± 0.82
	0.5	49.17 ± 13.85†	14.09 ± 4.45	45.44 ± 6.63	52.41 ± 15.78	1.25 ± 1.06	−0.46 ± 0.61
	1.0	48.73 ± 4.17	13.39 ± 2.55	44.42 ± 7.32	40.72 ± 10.81	1.08 ± 0.86	−0.47 ± 0.91
	2.0	39.59 ± 13.79	12.22 ± 3.83	36.83 ± 9.83	30.77 ± 26.34	2.98 ± 1.07	−0.72 ± 0.96

Values are given as means ± SD.
Values with the same superscript are significantly different ($p < .05$).
*$p = .031$; †$p = .031$; ‡$p = .03$.
IS-BIC, distance between implant shoulder and bone-implant contact; IS-BC, distance between implant shoulder and crestal bone.

Barros and colleagues[30] recorded maximum mineralization at 2 weeks and found pronounced differences in mineralization in comparison with nanomodified and microrough implants at even earlier stages, after 3 and 7 days, respectively.

Although the dynamics of bone formation were not generally affected in our study, we found a tendency for collagen II/CS to influence the mineralization rate (as indicated by the significantly higher amount of mineralized bone formed at week 4 compared with the control) and to significantly promote bone density, but this depended on the gap size. For both surface types, the degree of mineralization at each time point was lower for larger gaps and for greater distance to the surface. But comparing coated to uncoated surfaces after 4 weeks showed a significant increase of 26% for coated surfaces, compared with 19% for uncoated surfaces, in the case of no gap, while for a 2-mm gap no more difference could be observed (15% and 14%, respectively).

As mineralization is related to bone density, the same was found for this parameter. Gaps of 2 mm showed no difference in bone density for the two surface types, while collagen type II/CS-coated implants placed with 0.5-mm gaps or no gap showed a significantly higher bone density adjacent to the surface and a more coronal BIC, as evidenced by a lower IS-BIC distance. For no-gap implants, even the distant bone density was significantly higher for coated implants.

Apparently, the ECM coating does influence mineralization and bone density, but the effect is highest in the immediate vicinity and occurs only with no or very small intervening gaps. Though not statistically significant, the same was found to be true for BIC, which was also largest in sites with no gap and 0.5-mm gaps and decreased with increasing gap size.

The observed effects are in agreement with studies demonstrating that the coronal level of BIC is lower for larger peri-implant gaps above 0.5 mm[41] and with those showing increased levels of BIC after 4 weeks of healing in mandibular and maxillary bone for very similar implant coatings of collagen type I/CS.[5,18]

The effect on bone thus appears to be due to a release of effectors that stimulate mineralization in the immediate vicinity. The source of such effectors may either be cells that interact with the coating and as a consequence release such factors, or a release of coating components themselves, possibly due to cell-based coating degradation. The first possible reason may be a binding of cells via specific adhesion receptors to collagen type II, as osteoblasts have been shown to be able to distinguish between the fibrillar collagens found in mature and healing bone and respond with an increase in mineralization to the latter.[42] Also, various growth factors can interact with the glycosaminoglycan contained in the coating, which may potentiate their effect on cells.[43] The second possibility is a limited release of coating components. In this case especially, CS may have a positive effect on mineralization, as it is a molecule that has a high negative charge and can bind to collagen in the newly forming osteoid. Binding of the Ca^{2+} ions to the fibrils by CS may result in more nucleation sites, and thus more mineralization.

For vertical and horizontal bone apposition, we did not find any significant differences between the two surface types. Gap size did have an effect: Generally, the crestal bone level was lower for larger gaps, while for gapless implants crestal bone could even exceed the implant shoulder height. Horizontal bone apposition, a good indicator of gap-bridging capacity, showed that implants placed in larger gaps still had longer horizontal distances between the implant surface and bone even after the healing period, so that no positive effect of this ECM coating on gap bridging could be found.

A last consideration should be mentioned here with regard to the approach used in this study as a model for immediate implant placement. It is important to keep in mind that tooth extractions expose the lamina dura, which will then border the peri-implant gap. In the applied defect model, spongious bone is exposed instead, which will have different modeling and remodeling dynamics, and the response may differ.

Still, it can be concluded that the collagen type II/CS implant surface has a positive effect on the bone density, the mineralization rate, and to a degree, the BIC for short distances between host bone and the implant surface. Gap size likewise influences bone mineralization, density, and BIC but additionally has effects on vertical and horizontal bone apposition, all of which decrease with increasing gap size.

ACKNOWLEDGMENTS

We thank Heike Zimmermann and Marcel Arnold for excellent technical assistance. We further thank project partners of the SFB-Transregio 67 of the DFG (German Research Foundation), especially project A3. The study was supported by Dentsply-Friadent.

REFERENCES

1. Berglundh T, Abrahamsson I, Lang NP, Lindhe J. De novo alveolar bone formation adjacent to endosseous implants. Clin Oral Implants Res 2003; 14:251–262.
2. Terheyden H, Lang NP, Bierbaum S, Stadlinger B. Osseointegration – communication of cells. Clin Oral Implants Res 2012; 23:1127–1135.
3. Korn P, Schulz MC, Hintze V, et al. Chondroitin sulfate and sulfated hyaluronan containing collagen coatings of titanium implants influence peri-implant bone formation in a minipig model. J Biomed Mater Res A 2013. DOI: 10.1002/jbm.a.34913.
4. Schliephake H, Aref A, Scharnweber D, Bierbaum S, Sewing A. Effect of modifications of dual acid-etched implant surfaces on peri-implant bone formation. Part I: organic coatings. Clin Oral Implants Res 2009; 20:31–37.
5. Stadlinger B, Bierbaum S, Grimmer S, et al. Increased bone formation around coated implants. J Clin Periodontol 2009; 36:698–704.
6. Stadlinger B, Pilling E, Huhle M, et al. Influence of extracellular matrix coatings on implant stability and osseointegration: an animal study. J Biomed Mater Res B Appl Biomater 2007; 83:222–231.
7. Bierbaum S, Douglas T, Hanke T, et al. Collagenous matrix coatings on titanium implants modified with decorin and chondroitin sulfate: characterization and influence on osteoblastic cells. J Biomed Mater Res A 2006; 77:551–562.
8. Becerra-Bayona S, Guiza-Arguello V, Qu X, Munoz-Pinto DJ, Hahn MS. Influence of select extracellular matrix proteins on mesenchymal stem cell osteogenic commitment in three-dimensional contexts. Acta Biomater 2012; 8:4397–4404.
9. Chiu LH, Yeh TS, Huang HM, Leu SJ, Yang CB, Tsai YH. Diverse effects of type II collagen on osteogenic and adipogenic differentiation of mesenchymal stem cells. J Cell Physiol 2012; 227:2412–2420.
10. Kundu AK, Putnam AJ. Vitronectin and collagen I differentially regulate osteogenesis in mesenchymal stem cells. Biochem Biophys Res Commun 2006; 347:347–357.
11. Salasznyk RM, Williams WA, Boskey A, Batorsky A, Plopper GE. Adhesion to vitronectin and collagen I promotes osteogenic differentiation of human mesenchymal stem cells. J Biomed Biotechnol 2004; 2004:24–34.
12. Ballock RT, O'Keefe RJ. The biology of the growth plate. J Bone Joint Surg Am 2003; 85-A:715–726.
13. Kadler KE, Holmes DF, Trotter JA, Chapman JA. Collagen fibril formation. Biochem J 1996; 316(Pt 1):1–11.
14. Douglas T, Heinemann S, Bierbaum S, Scharnweber D, Worch H. Fibrillogenesis of collagen types I, II, and III with small leucine-rich proteoglycans decorin and biglycan. Biomacromolecules 2006; 7:2388–2393.
15. Douglas T, Heinemann S, Mietrach C, et al. Interactions of collagen types I and II with chondroitin sulfates A–C and their effect on osteoblast adhesion. Biomacromolecules 2007; 8:1085–1092.
16. Franz S, Rammelt S, Scharnweber D, Simon JC. Immune responses to implants – a review of the implications for the design of immunomodulatory biomaterials. Biomaterials 2011; 32:6692–6709.
17. Rammelt S, Illert T, Bierbaum S, Scharnweber D, Zwipp H, Schneiders W. Coating of titanium implants with collagen, RGD peptide and chondroitin sulfate. Biomaterials 2006; 27:5561–5571.
18. Stadlinger B, Hintze V, Bierbaum S, et al. Biological functionalization of dental implants with collagen and glycosaminoglycans – a comparative study. J Biomed Mater Res B Appl Biomater 2011.
19. Hammerle CH, Chen ST, Wilson TG Jr. Consensus statements and recommended clinical procedures regarding the placement of implants in extraction sockets. Int J Oral Maxillofac Implants 2004; 19(Suppl):26–28.
20. Meredith N. Assessment of implant stability as a prognostic determinant. Int J Prosthodont 1998; 11:491–501.
21. Botticelli D, Berglundh T, Buser D, Lindhe J. The jumping distance revisited: an experimental study in the dog. Clin Oral Implants Res 2003a; 14:35–42.
22. Chen S, Darby I, Adams G, Reynolds E. A prospective clinical study of bone augmentation techniques at immediate implants. Clin Oral Implants Res 2005; 16:176–184.
23. Botticelli D, Berglundh T, Buser D, Lindhe J. Appositional bone formation in marginal defects at implants. Clin Oral Implants Res 2003b; 14:1–9.
24. Bianchi AE, Sanfilippo F. Single-tooth replacement by immediate implant and connective tissue graft: a 1–9-year clinical evaluation. Clin Oral Implants Res 2004; 15:269–277.
25. Shibly O, Kutkut A, Albandar JM. One-year re-entry results of guided bone regeneration around immediately placed implants with immediate or conventional loading: a case series. J Int Acad Periodontol 2012; 14:62–68.
26. Berthod F, Saintigny G, Chretien F, Hayek D, Collombel C, Damour O. Optimization of thickness, pore size and mechanical properties of a biomaterial designed for deep burn coverage. Clin Mater 1994; 15:259–265.
27. Geiger M, Li RH, Friess W. Collagen sponges for bone regeneration with rhBMP-2. Adv Drug Deliv Rev 2003; 55:1613–1629.
28. Munting E, Wilmart JF, Wijne A, Hennebert P, Delloye C. Effect of sterilization on osteoinduction. Comparison of five methods in demineralized rat bone. Acta Orthop Scand 1988; 59:34–38.
29. Wolf-Brandstetter C, Lode A, Hanke T, Scharnweber D, Worch H. Influence of modified extracellular matrices on Ti6Al4V implants on binding and release of VEGF. J Biomed Mater Res A 2006; 79:882–894.

30. de Barros RR, Novaes AB Jr, Queiroz A, de Almeida AL. Early peri-implant endosseous healing of two implant surfaces placed in surgically created circumferential defects. A histomorphometric and fluorescence study in dogs. Clin Oral Implants Res 2012; 23:1340–1351.
31. Donath K, Breuner G. A method for the study of undecalcified bones and teeth with attached soft tissues. The Sage-Schliff (sawing and grinding) technique. J Oral Pathol 1982; 11:318–326.
32. Wennerberg A, Albrektsson T. On implant surfaces: a review of current knowledge and opinions. Int J Oral Maxillofac Implants 2010; 25:63–74.
33. Mohamed S, Polyzois I, Renvert S, Claffey N. Effect of surface contamination on osseointegration of dental implants surrounded by circumferential bone defects. Clin Oral Implants Res 2010; 21:513–519.
34. Rossi F, Botticelli D, Pantani F, Pereira FP, Salata LA, Lang NP. Bone healing pattern in surgically created circumferential defects around submerged implants: an experimental study in dog. Clin Oral Implants Res 2012; 23:41–48.
35. Covani U, Bortolaia C, Barone A, Sbordone L. Bucco-lingual crestal bone changes after immediate and delayed implant placement. J Periodontol 2004; 75:1605–1612.
36. Polyzois I, Renvert S, Bosshardt DD, Lang NP, Claffey N. Effect of Bio-Oss on osseointegration of dental implants surrounded by circumferential bone defects of different dimensions: an experimental study in the dog. Clin Oral Implants Res 2007; 18:304–310.
37. Carlsson L, Rostlund T, Albrektsson B, Albrektsson T. Implant fixation improved by close fit. Cylindrical implant-bone interface studied in rabbits. Acta Orthop Scand 1988; 59:272–275.
38. Schenk RK, Willenegger HR. [Histology of primary bone healing: modifications and limits of recovery of gaps in relation to extent of the defect]. Unfallheilkunde 1977; 80:155–160. In German.
39. Liu Y, Chan JK, Teoh SH. Review of vascularised bone tissue-engineering strategies with a focus on co-culture systems. J Tissue Eng Regen Med 2012. DOI: 10.1002/term.1617.
40. Alford AI, Hankenson KD. Matricellular proteins: extracellular modulators of bone development, remodeling, and regeneration. Bone 2006; 38:749–757.
41. Knox R, Caudill R, Meffert R. Histologic evaluation of dental endosseous implants placed in surgically created extraction defects. Int J Periodontics Restorative Dent 1991; 11:364–375.
42. Bierbaum S, Hempel U, Geissler U, et al. Modification of Ti6Al4V surfaces using collagen I, III, and fibronectin. II. Influence on osteoblast responses. J Biomed Mater Res A 2003; 67:431–438.
43. Hintze V, Moeller S, Schnabelrauch M, et al. Modifications of hyaluronan influence the interaction with human bone morphogenetic protein-4 (hBMP-4). Biomacromolecules 2009; 10:3290–3297.